International Journal of Agriculture, Environment and Biotechnology
Citation: *IJAEB*: **16**(04): 253-265, December 2023
DOI: 10.30954/0974-1712.04.2023.4

ASSOCIATION FOR AGRICULTURE ENVIRONMENT AND BIOTECHNOLOGY

RESEARCH PAPER

Production and Characterization of Biochar Produced from Batch Slow Pyrolysis of Millet Straw

I. Abubakar* and M.D. Saeed

Department of Pure and Industrial Chemistry, Faculty of Physical Sciences, Bayero University Kano, PMB, Kano, Nigeria

*Corresponding author: kainuwailiyas@gmail.com (**ORCID ID:** 0009-0000-0494-6897)

Paper No. 1098 **Received:** 07-09-2023 **Revised:** 01-11-2023 **Accepted:** 30-11-2023

ABSTRACT

Agricultural waste is a vital renewable resource that promotes environmental sustainability, global economic growth, and energy security. The focus of this study is on the effect of pyrolysis temperature on physicochemical properties of biochar derived from millet straws as an agricultural wastes pyrolyzed at four different pyrolysis temperatures of 300, 400, 500 and 600 ◦C for 30, 60, 90, and 105-minutes residence time, respectively. The produced biochars were characterized by proximate and ultimate analysis, Brunauer–Emmett–Teller (BET), X-ray diffraction (XRD), and Fourier transform infrared spectroscopy (FTIR). Pyrolysis temperature was shown to have a strong influence on physicochemical characteristic of biochar samples. The experimental data shows that as pyrolysis temperature increased, ash content, pH, electrical conductivity, cation exchange capacity, fixed carbon, BET surface area, and total C content increased while biochar yield, total content of O, H and S significantly decreased. Similarly, the ratios of O/C, H/C, tended to decrease with the upsurge of pyrolysis temperature. The FTIR data indicated an increase in aromaticity and a decrease in polarity of biochar produced at a high temperature. Meanwhile, the XRD showed that with increased in pyrolysis temperature, cellulose component of biomass loss and crystalline mineral components increased. The result suggest that biochar produced at higher pyrolysis temperatures possess stable carbon, which can be used to sequester carbon when used as soil amendment.

HIGHLIGHTS

- Millet straws biochar was produced from the batch pyrolysis at different temperatures of 300, 400, 500, and 600.
- The produced biochars were characterized for proximate, and ultimate analysis, as well as the BET, FTIR and XRD analyses for surface area, functional groups, and crystalline nature the biochars, respectively.
- Pyrolysis temperature was found to have significant effect on the physicochemical properties of the biochar.
- Base on the physicochemical properties of millet straws biochar, the millet straws biochar could be a source of soil amendment, in carbon sequestration, as an adsorbent for organic and inorganic contaminants from the environments.

Keywords: Millet straw, biochar, pyrolysis, physicochemical properties

Agricultural waste is a vital renewable resource that promotes environmental sustainability, global economic growth, and energy security. Since forestry and agriculture account for the majority of the economies of developing countries, it is extremely desirable to utilize this biomass (El-hassanin *et al.* 2020). The majority of these wastes are biomass, which has a massive energy content. Regrettably, these wastes are not effectively utilized or manage, particularly in developing countries (Aruya *et al.*

How to cite this article: Abubakar, I. and Saeed, M.D. (2023). Production and Characterization of Biochar Produced from Batch Slow Pyrolysis of Millet Straw. *Int. J. Ag. Env. Biotech.*, **16**(04): 253-265.

Source of Support: None; **Conflict of Interest:** None

2016). Large amounts of agricultural residues are produced and subsequently abandoned as wastes (Song *et al.* 2023). The accumulation of these wastes that is continuously produced has been causing environmental problems. It has been reported that during harvest season, over 25% of crop straws are burned to remove crop residues, which is harmful for human health and air quality (El-hassanin *et al.* 2020). In light of the United Nation's sustainable development goals, which prioritize improved public health and environmental sustainability, a more effective strategy for handling agricultural waste must be developed so that it can be properly disposed of or converted into useful products. (Oyegoke *et al.* 2023). The use of agricultural wastes to produced biochar for different application has continue to attract the attention of many scholars (Kammann *et al.* 2017; Khawkomol *et al.* 2021; Mahanty & Mondal, 2021; Wahi *et al.* 2015). To produce a solid, liquid, or gaseous fuel, conversion processes can be thermal, chemical, biological, or physical. Thermochemical synthesis of biochar appears to be the most promising option. One of the most effective methods for making biochar is the pyrolysis of biomass (Biswas *et al.* 2017). Pyrolysis, a process, which involves rapidly heating feedstock to moderate temperatures with or without the presence of oxygen or air (Wystalska & Meers, 2021). The main products of pyrolysis of biomass are biochar, bio-oil, and gases (Jiang *et al.* 2019). The production of biochar mostly dependent on the operating conditions during pyrolysis. Biochar generated at higher temperatures has a greater porous surface area and lower O/C and H/C ratios, which improves its ability to adsorb organic and inorganic pollutants. However, since they include more oxygen-containing functional groups, biochars made at lower temperatures have superior heavy metal adsorption properties in wastewater in addition to conserving energy (Hu *et al.* 2022). Biochars are porous carbonaceous materials produced from biomass pyrolyzed under high temperatures of 300–700 ◦C in the absence or presence of insufficient air (Nazari *et al.* 2019). Biochar production depend upon the technique employed to it production as well as the process parameters involved during the production process (Tripathi *et al.* 2016). Biochars are considered as important materials in various environmental applications such as carbon sequestration, greenhouse gas reduction, soil fertilization, and wastewater treatment (Almeida *et al.* 202,). As well as an excellent form of adsorbents due to the fact that it typically required little or no treatment, couples with abundance functional groups, such as hydroxyl groups, carboxyl groups, and phenols, and large surface area (Loulidi *et al.* 2020). Sustainable agricultural waste disposal has continue to gained the global attention as environmentally friendly technique in recent years (Sahoo *et al.* 2021a). Agricultural residues such as sugarcane bagasse (Almeida *et al.* 2022), peanut shells (Natrayan et al., 2022), corn straw (Fan *et al.* 2018), rice straw (Nguyen *et al.* 2019) and black tea wastes etc. (Ullah *et al.* 2022). That contain cellulose, hemicellulose and lignin, are abundant sources of carbonaceous materials (Mubarik *et al.* 2015). However, the production of biochar from this crop residues by pyrolysis is one of the most promising techniques (Burachevskaya *et al.* 2023). Meanwhile, the physicochemical properties of biochars vary significantly with the pyrolysis conditions and type of crop residue. While the former is considered to have greater influence on the final properties of the biochar (Dhyani & Bhaskar, 2017). The aimed of this study is to investigate the effects of slow batch pyrolysis temperatures on the yields, morphology and physicochemical properties of biochar produced from millet straws agricultural waste.

MATERIALS AND METHODS

Samples collection and treatment

The millet straws were collected from the local farm land, which was used as feedstocks for the preparation of the biochars in this study. Prior to the experiments, the feedstocks were air dry for 30 days. For better exposure to heat during slow pyrolysis in the muffle furnace feedstocks were cut into small pieces of around 5-6 cm in length. Afterward, the biomass materials were washed with distilled water to remove any dirt and dust before drying in an oven dried (thermostat oven DHG-9023A) for 24 h at 105°C before pyrolysis (Sahoo *et al.* 2021a).

Preparation of biochar

The oven dried millet straws were subjected to a batch slow pyrolysis in a muffle furnace (Carbolite Gero-30-3000°C, UK). Placed in a ceramic crucible, covered with a tightly fitting lid and wrapped with

aluminium foil sheet, and then placed in the muffle furnace and heated to 300, 400, 500, and 600 °C, at a constant heating rate of 10°C/min for 30-, 60-, 90, and 105-mins residence time respectively. The furnace was switched off after the set temperature and allowed to cooled for some time before taken out from the furnace and cooled in a desiccator to room temperature, The biochars were then, crushed and passed through a 100-mesh sieve and stored in airtight plastic containers for subsequent analysis. The biochars produced from the straws at 300, 400, 500, and 600 °C was designated as BCM-300, MBC-400, BCM-500, and BCM-600, respectively (Wei *et al.* 2019).

Biochar yield

The yield of biochar is expressed as the ratio of the mass of the biochar to the initial mass of the feedstock subjected to the pyrolysis process (Sahoo *et al.* 2021b).

$$\text{Biochar yield \%} = \frac{\text{Mass of Biochar}(g)}{\text{Oven dry mass of feed stock}}$$

Characterization of biochar samples

The biochar samples were characterized to observe the effect of pyrolysis temperatures on the crystallography, functional groups characterizations, BET analysis, physical and chemical characterization. The proximate characterization was conducted as per the standard D1762 – 84, to determine moisture, volatile matter, ash content of biochar samples (Aller *et al.* 2018). For moisture content determination, approximately 1 g of air-dried biochar was weighed into a ceramic crucible and heated for 2 hours samples. MC was determined based on mass loss after two hours at 105 ◦C (Sahoo *et al.* 2021a). Volatile matter determination was conducted as (Sahoo *et al.* 2021b). 1 g of the dried biochar samples each was heated at 950 ◦C for 7 min in a muffle furnace. However, 1g each of the biochar samples were placed into a lid covered crucible and combusted at 750°C for 6 h in a muffle furnace (Liu *et al.* 2018) for ash content determination. The percentage fixed carbon was determined by the difference in sum of moisture, volatile matter and ash from 100. The fractions of C, H, N, and S was determined by ultimate analysis in a CHNS Elemental analyzer in the biochar samples. However, the mass fractions of oxygen were calculated by the difference (Campos *et al.* 2020). The pH and EC of the biochar samples were determined using digital pH meter. A 1g each of biochars were mixed with 10 mil distilled water and Shaked for 1 h on a reciprocating shaker at 35.5°C (Aller *et al.* 2018). The cation Exchange Capacity (CEC) was determined according to the procedure adopted by (Baffi & Cassinari 2010). Briefly, 5 g each of the biochar samples were mixed with 40 ml of 1.0 moldm^3 ammonium acetate solution (pH 7) in 100 mil plastic beaker and stirred with glass rod and left overnight. It was the suction-filtered with 55 mm Buchner funnel. The residue from filtration was leached with four 25ml portions of 1 moldm^3 NH4Cl solution (pH 7). The solution was discarded and the electrolyte washed out of the sample with 150 ml ethanol. The sample was allowed to drain completely and leached gradually with acidified NaCl to 250 ml. 50 ml of 2% boric acid was measured into 250 ml comical flash and 3 drops of mixed indicator were added. The acidified NaCl leachate was poured into 500 ml Kjeldahl flask and 10 ml of 1.0 moldm^3 NaOH and anti-bumping granules were added. The leachate was distillates over the boric. 1.5 ml of ammonium borate distillate was titrated with standard 0.1 moldm3 HCl. For the BET surface area of biochars were measured using a NOVA 4200e analyzer (Quantachrome Instruments, USA) at liquid nitrogen temperature (77 K). The Brunauer–Emmett–Teller (BET) surface area (SBET), micropore surface area (S_{mic}) and micropore volume (V_{mic}) of the biochars produced at different temperatures were determined using the BET equation, t-plot method and single point adsorption total pore volume analysis, respectively (Zhao *et al.* 2017). The functional groups present in the biochars were characterized by FTIR spectrometer (PE-1710, USA). Dried biochar. Approximately 10mg of each of the samples were dispersed in 200mg of spectroscopic grade KBr to record the spectra using potassium bromide disks to prepare the biochar samples. The spectral range from 4000 – 650 cm^{-1} (Liu *et al.* 2012). The mineral compositions of the biochars and biochar composites samples were analyzed using X-ray diffraction (XRD). The XRD was used to identify the crystalline phases formed for the prepared biochars, using the diffractometer (Bruker D8 Advance), equipped with the Kα radiation of copper (λ = 1.5406) produced at 45kV

15mA, the data were collected over 2θ range (0–80°) at 2θ scan rate of 10°min^{-1}.

STATISTICAL ANALYSIS

Except BET analysis, all other experimental data were expressed as means of three replicates. One-way analysis of variance (ANOVA) experimental data were conducted in this work using the MINITAB software, and the Turkey's HSD post-hoc tests ($p < 0.05$) were used to identify significant differences among different biochar (Zhang *et al.* 2022).

RESULTS AND DISCUSSION

Biochars Yields

The results of the biochar yields from millet straws at different pyrolysis temperatures is presented in table 1. It can be observed from the table that, there is a significant ($p < 0.05$) decreased in biochar yield with the corresponding increase in pyrolysis temperatures. The percentage yield of BCM declined from 48.33 to 28.58%, when the temperature rose from 300 to 600°C respectively. This results are in agreement with the previous research conducted by various scholars. (Liu & Fan 2018) reported that, the yield of biochar derived from wheat straw declined from 35.9 to 23.9% when the temperature rose from 300 to 700 respectively. Moreover, (Cheng *et al.* 2021) reported that the yield of cotton stalk biochar decreased from 46.71 to 33.15 %, when the pyrolysis temperatures was increased from 300 to 500 ◦C, respectively. Additionally, (Zhao *et al.* 2017) demonstrated that, increased in pyrolysis temperatures from 300 to 500 ◦C, the yield of biochar derived from apple tree branches respectively decreased from 47.94 to 31.71%. This significant declined in the biochar yield may be attributed to lost in mass, principally due to loss in moisture and hydrated water, and decomposition and transformation of complex organic compounds into vapor mixed with gases such as water vapor, CO_2, CO, H_2, CH_4, and heavier hydrocarbons (Hmid *et al.* 2014a; Novak, 2014; Sun *et al.* 2014). However, the main components of these straws are hemicellulose, cellulose, and lignin, and their decomposition temperatures are in the ranges of 315– 400, 220–315, and 160–900 °C, respectively (Liu & Fan, 2018).

Table 1: Millet straws biochar yields

Biochars	Pyrolysis temperature (°C)	Heating rate (°C/ min)	Residence time (min)	Yields (%)
BCM-300	300	10	30	48.33 ± 0.020[a]
BCM-400	400	10	60	40.67 ± 0.520[b]
BCM-500	500	10	90	34.45 ± 0.514[c]
BCM-600	600	10	105	28.58 ± 0.020[d]

Note: Each value represents the mean of three replicates (n=3), ± standard deviation. Small letters following the numerical values denote significant differences between each row data ($p < 0.05$). However, means that do not share a letter are significantly different.

Physical and ultimate analysis of biochar

The proximate analysis of derived biochars at pyrolysis temperatures of 300, 400, and 600 is summarized in table 2. As expected, these results were largely dependent on pyrolysis temperatures. The volatile matter and moisture content from the results showed that increased in pyrolysis temperature significantly ($p<0.05$) decreased the volatile matter and moisture content for all the biochars produced. The percentage volatile matter of the derived biochar diminished gradually from 83.04 to 36.03%, when the pyrolysis temperature increased from 300 to 600, respectively. This finding is consistent with results obtained by many researchers using different feedstocks. (Xin Zhang *et al.* 2022) using sewage sludge biochars, (Venkatesh *et al.* 2013), with cotton stalk biomass. (Steiner *et al.* 2009) from peanut hulls, pecan shells, poultry litter, and switchgrass. However, this gradual decreased in volatile matter of the biochar produced at higher pyrolysis temperature is attributed to a greater loss of gaseous products and low molecular mass hydrocarbons (such as CH_4, C_2H_6, and C_3H_8 (Gaffar *et al.* 2021). The percentage ash content obtained (table 2) across all the biochars increased significantly ($p<0.05$) as the highest pyrolysis temperature (600). Such increased in ash content with increased in pyrolysis temperature have been observed previously (Cuixia *et al.* 2020; Reyhanitabar *et al.* 2020; Song *et al.* 2023; Videgain-marco *et al.* 2020; Zhang *et al.* 2023). This is due to the gradual concentration of inorganic components and the reduction of other elements during pyrolysis. Thus,

representing the inorganic portion that cannot be volatilized or degraded by combustion (Almeida *et al.* 2022; Hadey *et al.* 2022). (Hu *et al.* 2022) reported that the ash content of biochar produced from maize straw increased from 21.31% to 24.54% with the increased in pyrolysis temperature from 300 to 500 ◦C. rose in pyrolysis temperature, resulted in the increased in concentrations of minerals and the combustion residues of organic matter and this lead to the increased the adsorption behaviour of biochar (Natrayan *et al.* 2022). The fixed carbon content also shows a positive correlation with the increased in pyrolysis temperature. It can be observed from table 2 that BCM-600 demonstrated higher fixed carbon of 52.50% at highest pyrolysis temperature of 600. This is mainly due the fact that the overall biochar mass reduces at higher pyrolysis temperature (Gaffar *et al.* 2021). This finding is in total agreement with the result of (Dhar *et al.* 2020; Guo *et al.* 2021). Fixed carbon content play a vital role for the carbon sequestration ability of the biochars (Dhar *et al.* 2020). mainly because a higher pyrolysis temperature can reduce overall biochar mass.

Table 2: Proximate analysis of millet straws biochar

	Parameters (%)			
Samples	**Moisture content**	**Volatile content**	**Ash content**	**Fixed carbon**
BCM-300	6.6±0.40a	83.04±0.05a	3.6±0.10c	6.76±0.09d
BCM-400	2.0±0.08b	78.01±0.02b	4.6±0.05b	15.39±0.13c
BCM-500	1.8±0.09b	66.03±0.95c	4.9±0.04b	27.27±0.01b
BCM-600	1.7±0.02b	36..03±0.10d	7.0±0.04a	55.27±0.2a

Analysis of millet straws biochar

The results of the ultimate analysis are presented in table 3. BCM-600 derived biochar gave the highest mass fraction of carbon of 49.82% at pyrolysis temperature of 600 ◦C. And higher carbon content in biochar, could be used as a source of carbon materials (Guo *et al.* 2021). This result showed similar trend with the previous results obtained by (Adekanye *et al.* 2022; Almeida *et al.* 2022; Poo *et al.* 2018; Sun *et al.* 2023; Xiaoxiao *et al.* 2019; Zhao *et al.* 2017). However, contrary to the carbon content, the hydrogen (H) oxygen (O), and nitrogen contents (table 3) had a negative correlation with significant difference ($p<0.005$), with the sequential increased in pyrolysis temperature for all the biochars. (Hmid *et al.* 2014b) report similar trend with olive mill waste. That, H decreased from 4.97% to 1.89%, O declined from 15.90% to 3.51% and N reduced from 1.02% to 0.73%, when the pyrolysis temperature rose from 430 to 530, respectively. This effect of pyrolysis temperature occurred due to the loses of surface functional-OH groups, C-bond, O and H atoms during the pyrolysis process of the feedstock owing to dehydration and structural core degradation at higher temperatures (Mahanty & Mondal, 2021; Steiner *et al.* 2009). In the meantime, the H/C and O/C molar rations, are the main parameters that are generally used to characterize the degree of organic aromaticity of the biochar (Wang *et al.* 2018; Xin Zhang *et al.* 2022). From (table 3) it can be observed that both H/C and O/C molar rations of all the biochars produced decreased significantly with increasing pyrolysis temperature. These strong negative correlation with increased in pyrolysis temperatures is attributed to the decarboxylation and decarbonylation during pyrolysis (Zhenyu *et al.* 2013). However, the C/N ratio significantly ($p<0.05$) rose with the increased in pyrolysis temperatures, indicating to the N ratio decreased faster than that of C, as well as the reduction of nitrogen-containing functional groups. This result was in agreement with the research of (Xin Zhang *et al.* 2022) that, the C/N ratio of biochar derived from sewage sludge increased from 5.74 to 8.61% when the temperature increased from 300 to 700, respectively.

Table 3: ultimate analysis of millet straws biochar

	Parameters							
Samples	**C (%)**	**H (%)**	**O (%)**	**N (%)**	**S (%)**	**H/C**	**O/C**	**C/N**
BCM300	43.96±0.12a	5.70±0.09a	44.28±0.10a	2.46±0.02a	4.59±0.03a	1.55	0.76	20.80
BCM400	44.52±0.08b	5.53±0.10a	43.33±0.15b	2.02±0.02b	10.33±0.02b	1.48	0.75	25.69
BCM500	48.12±0.06c	5.29±0.121a	39.99±0.09c	1.90±0.02bc	4.36±0.09c	1.30	0.62	29.52
BCM600	49.82±0.11c	4.96±0.17a	36.43±0.02d	1.79±0.02c	7.33±0.02c	1.19	0.55	32.45

Chemical analysis of biochar

pH and EC

It has been reported that increased in pyrolysis temperature generally raised the pH and EC of biochar and that the pH of biochars are generally alkaline (Conz *et al.* 2017; Guo *et al.* 2021; Poo *et al.* 2018). However, this study recorded similar trend, that increased in pyrolysis temperature increased the pH of all the biochars generated as shown in table 4. The pH increased from 7.45 to 10.39 with the increased in pyrolysis temperatures from 300 to 600, respectively. The high pH of the biochar may attributed major ash components such as K^+, Na^+, Ca^{2+}, Mg^{2+}, HCO_3^-, and CO_3^{2-} (Song & Guo 2012). (Song *et al.* 2023) reported that increased in the pyrolysis temperature increased the pH of pineapple leaves, banana stems, sugarcane bagasse and horticultural substrate from 7.17 to 7.51, and from 8.89 to 9.77 from 300 to 700 respectively. (Bera *et al.* 2017; Tran *et al.* 2016) demonstrated higher pH to the present of organic functional groups and inorganic minerals resulted from carbonization of feedstocks at higher pyrolysis temperature, and functional groups such as –COO– and –O– groups in biochars, were involved in protecting the acid reaction hence, contributed to the alkalinity of the biochars through association of these groups with H the alkaline pH of biochars. However, there is also increased in Electrical Conductivity (EC) with an increased in pyrolysis temperature as depicted in table 4.

Table 4: Chemical properties of millet straws biochar

Samples	Parameters		CEC (cmol/kg)
	pH	EC (dS/m)	
BCM-300	7.45±0.01c	4.50±0.12d	28.60±0.02a
BCM-400	9.57±0.01b	7.43±0.03c	64.40±0.02b
BCM-500	10.48±0.03a	13.87±0.01b	71.11±0.02c
BCM-600	10.39±0.05a	16.12±0.02a	75.60±0.21d

As shown in the table 4, increased in pyrolysis temperatures, had significantly ($P<0.05$) increased the EC. The EC of millet straw biochar increased from 4.50 to 16.12 dS /m at pyrolysis temperature of 300 to 600respectively. This positive correlation may be connected to the increased in ash content in biochars with the increased in pyrolysis temperature resulting in greater of loss of organic acidic portion in biochar with constant increased in the amount of ions present through the increase in ash content (Askeland *et al.* 2019; Bera *et al.* 2017). This finding is in agreement with results reported by (Reyhanitabar *et al.* 2020) with Tea waste, Wheat straw husk, Apple tree wood pruning waste, and Walnut derived biochars.

Cation Exchange Capacity (CEC)

The cation exchange capacity (CEC) is the amount of exchangeable cations such as Ca^{2+}, Mg^{2+}, K^+, Na^+, NH_4^+ that a material is capable of holding (Weber & Quicker, 2018). Table 4 presented the CEC of the millet straw biochars produced. The increased in pyrolysis temperatures from 300 - 600 significantly increased the CEC of the biochars ($p<0.05$). The CEC of BCM increased from 28.60 to 75.60 cmol/kg, at 300 to 600, rise in temperatures, respectively. Similar trend was obtained by (Wystalska & Meers 2021) with poultry manure biochar. The increase in cation exchange capacity (CEC) indicates the addition of electrolyte content in substances, and the increase of electrolyte content can promote the ion exchange between adsorbents and heavy metals (Wystalska *et al.* 2023).

BET Specific Surface Area

BET analysis was used to determine the specific surface area of pyrolyzed millet straws. The specific surface area, pore volume and pore diameters of the biochars are given in table 5. From table, it was observed that, the specific surface area (SSA) and pore volume of the millet straws biochars increased from 281.992 to 404.284 m^2/g and 0.173 to 0.216 cc/g with increased in pyrolysis temperatures from 300 to 600, respectively. This result is in agreement with findings of (Ahmad *et al.* 2012; Amin *et al.* 2017; Fan *et al.* 2020; Sahoo *et al.* 2021b; Wu *et al.* 2019). The surface area increased of biochar derived from coconut fibers from 193.7 to 278.58 m^2/g with the pyrolysis temperature increased from 450 to 500 °C was also reported by (Dhar *et al.* 2020). However, this positive correlation of surface area of biochars with increased in pyrolysis temperature could be attributed to the complete devolatilization of the original biomass components (cellulose, hemicellulose and lignin), and removal of pore-blocking substances, destruction of aliphatic alkyls and ester groups, exposure of the aromatic lignin

core, thermal cracking and formation of vesicular bundles or channel structures (Gaffar *et al.* 2021). Higher surface area biochars are considered as potential adsorbent (Xiaoling *et al.* 2020).

Table 5: BET analysis of millet straws biochar

Samples	BET Surface Area (m^2/g)	Pore Volume (cc/g)	Pore diameter (nm)
BCM-300	281.992	0.173	2.132
BCM-400	334.666	0.168	2.100
BCM-500	347.909	0.216	2.144
BCM-600	404.284	0.224	2.123

Fourier transform infrared spectroscopy (FTIR) Analysis

The analysis of the FTIR spectrum shows the presence of many peaks in the range of wavenumbers from 4,000 to 1000cm^{-1} indicating the complex nature of millet straw biochar (Bayu *et al.* 2019; Loulidi *et al.* 2020). The spectra of the biochar prepared at pyrolysis temperatures of 300, 400, 500 and 600 were presented in Fig. 1 and the functional groups involved in the structures of the biochars are also provided in table 6. From the Fig. 1 it can be observed that pyrolysis temperature has greater influence on the biochar surface functional groups. The adsorption peaks at 2922 cm^{-1} in the BCM-300, which is attributed to aliphatic C-H group (Azlina *et al.* 2013; Ertugay & Malkoc, 2014; Huang *et al.* 2021; Yaoyao *et al.* 2019), and this confirms the presence of aliphatic hydrocarbon (Natrayan *et al.* 2022), found in cellulose and hemicellulose (Munar-florez *et al.* 2021) has disappeared when the temperature raised. However, the peak at 3755 cm^{-1} was observed in BCM-500, and this was ascribed to the stretching vibration of the phenolic or alcoholic hydroxyl groups (-OH) (Bayu *et al.* 2019; Coates, 2000; Gao *et al.* 2023; Tong *et al.* 2011). The bands between 2178cm^{-1} to 2163cm^{-1} are also present, which is attributed to Thiocyanate (-SCN) (Bayu *et al.* 2019). Furthermore, the peaks between 2117cm^{-1} to 2113 cm^{-1} was ascribed to the presence of C≡C stretching vibration of terminal alkyne. And /or were attributed to ketene (C=O) groups (Song *et al.* 2023). The bands between 1580 to 1509cm^{-1} were found between BCM-300 and BCM-400 biochars indicating a weak aromatic ring stretch (C=C) (Fan *et al.* 2018; Mary *et al.* 2016). contained in the lignin structure (Almeida *et al.* 2022). The band at 1420 cm^{-1} was attributed to the stretching vibration of C = O in lignin (Sarfaraz *et al.* 2020; Xing *et al.* 2018), and/or indicative of bending vibration of O-H in carboxylic acid (P. Zhang *et al.* 2020). The peaks at between 1369 to 1362 cm^{-1} in BCW-300

Table 6: Main FTIR Peaks for the functional groups of the millet straw biochars

BCM-300		**BCM-400**	
Wavenumbers (cm^{-1})	**Functional groups**	**Wavenumbers (cm^{-1})**	**Functional groups**
2922	Methylene C-H asym./sym. stretch	2113	C≡C Terminal alkyne
2178	Thiocyanate (-SCN)	2063	Aliphatic –C==C–, C==O of aliphatic aldehyde
2113	C≡C Terminal alkyne	1576	Aromatic C=C ring stretch
1988	Isothiocyanate (-NCS)	1377	Aromatic tertiary amine stretch
1580	Aromatic C=C ring stretch	872	Out-of-plane aromatic C–H bending
1509	C=C-C Aromatic ring stretch	779	Out-of-plane aromatic C–H bending
1097	Aliphatic ether C–O and alcohol C–O stretching	693	Si-O- and/or Aliphatic bromo compound, C-Br stretch
782	Out-of-plane aromatic C–H bending		
BCM-500		BCM-600	
Wavenumbers (cm^{-1})	**Functional groups**	**Wavenumbers (cm^{-1})**	**Functional groups**
3755	Primary or secondary, OH in-plane bend	2117	C≡C Terminal alkyne
2105	C≡C terminal alkyne mono-substituted	1992	Isothiocyanate (-NCS)
1988	Isothiocyanate (-NCS)	1917	Isothiocyanate (-NCS)
1563	Aromatic C=C ring stretching	1397	$-CH_3$ Trimethyl or tert-butyl
1397	Methyl C-H asym. /sym. bend	872	Si–O–Si groups
875	Si–O–Si groups	693	Si–O– groups/ aromatic C–H out-of-plane
689	Si–O– groups/ aromatic C–H out-of-plane		

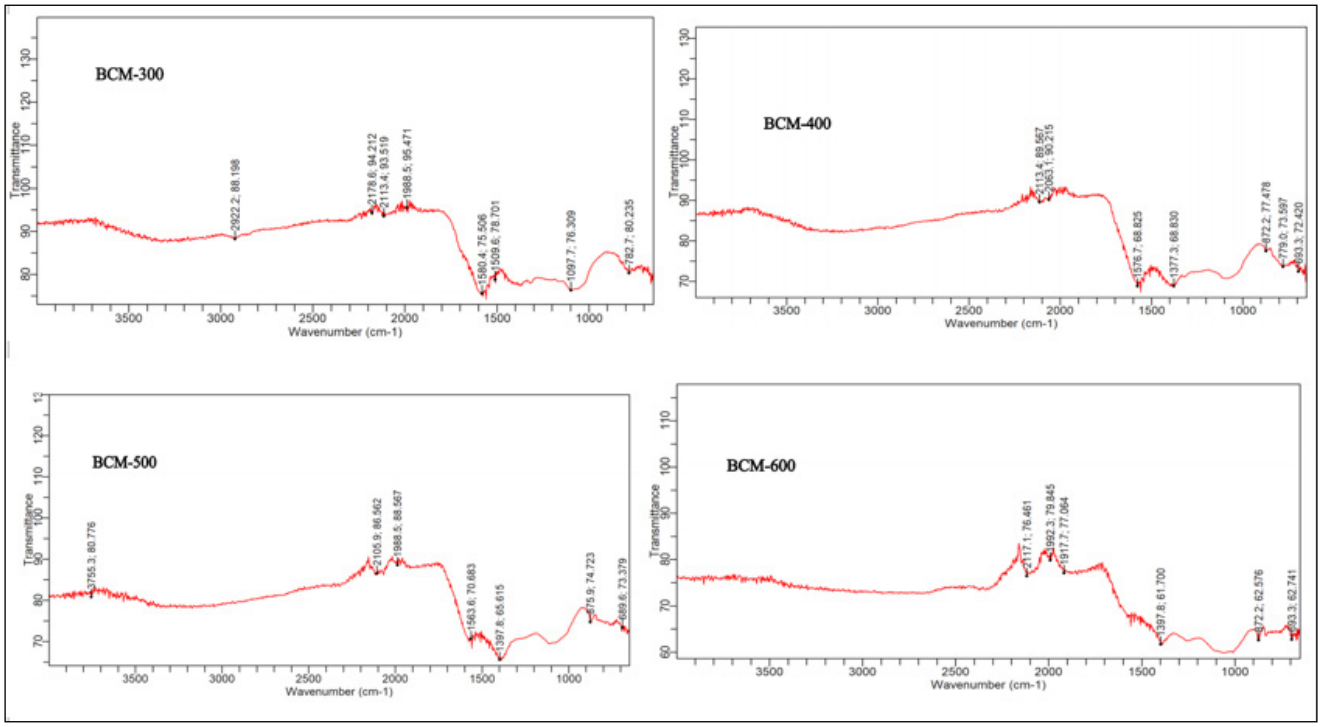

Fig. 1: FT-IR Spectrum for millet straw biochars produced at different pyrolysis temperatures

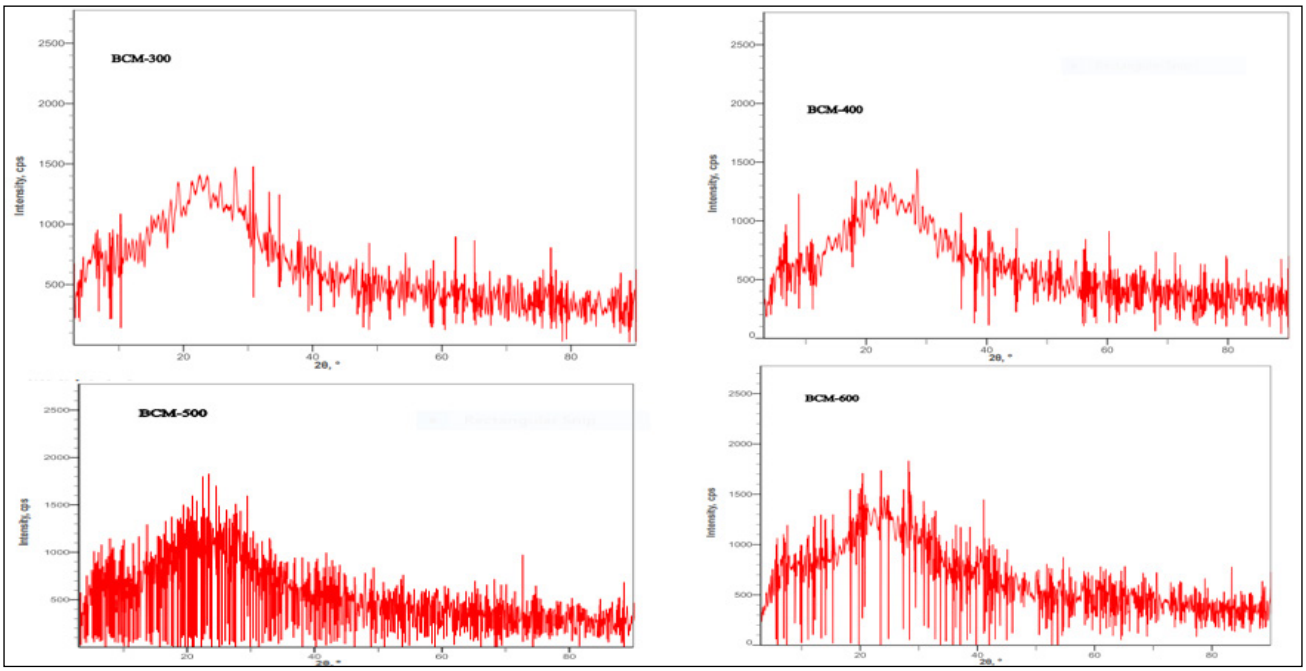

Fig. 2: XRD Analysis of millet straw biochars produced at different pyrolysis temperatures

and BCW-400 indicate the presence of C–O group of carboxyl and alcohol of lignin (Khawkomol *et al.* 2021). The peaks at 1065 cm^{-1} was due to the stretching of C–O–C (Khawkomol *et al.* 2021; Xing *et al.* 2018). The peaks at 1097 is assigned to phenolic OH and aromatic C–O bonds (Ali *et al.* 2022). The band at 875 cm^{-1} is ascribed to stretching of Si–O–Si groups (Khawkomol *et al.* 2021; Xing *et al.* 2018). The bands at 875 to 872 present in all the biochars is characterized by out-of-plane aromatic C–H bending vibrations (Keerthanan *et al.* 2020). The peaks at 782 to 779 cm^{-1} which were observed typically in all the prepared biochars represent Si-O-Si group (Shi *et al.* 2019). This is due to the abundant

Si in straws of the feedstocks. The bands at 693 to 689cm^{-1} designed for the aromatic C–H out-of-plane vibration and/or the Si-O band (Singh *et al.* 2023).

X-ray diffraction (XRD) Analysis

XRD analysis was used to evaluate the degree to which the samples were crystalline or amorphous. The XRD characteristics of the biochars are presented in Fig. 2. The samples were analyzed in the region of 2 Theta (θ) and angle range of 0°- 80° at room temperature. The characteristic peaks in the XRD pattern for all the biochars generated indicated the presence of five peaks at 2 of 19.5, 21.37, 43.2, 50.6 and 80.2. The peak at 2θ = 21.37 is characterized by presence of inorganic minerals such as SiO_2 (El-hassanin *et al.* 2020; Naeem *et al.* 2019). And is an indication that the biochars were amorphous carbon. Additionally, the peaks revealed the presence of graphene structure in all biochar samples (Amen *et al.* 2020). The formation of graphene structures can occur during the pyrolysis of materials derived from agricultural by-products (Le *et al.* 2021). The identification of another band within the range of 43.2 at an angle of 2θ can be assigned to the layers of the graphene oxide layer in a short-ranged order form and the appearance of peaks of 50.70° and 81.2 at 2θ may be attributed to calcite, (Ampofo *et al.* 2021). conclusively, it can be said that the biochars produced from the straws are mainly composed of the amorphous carbon due to the absence of any strong and sharp peak in the XRD (Amen *et al.* 2020). When a substance is crystalline, well-defined peaks can be observed, whereas non-crystalline or amorphous materials exhibit hollow peaks. Additionally, a highly sharp and strong peak shows that the material has developed a pure crystalline structure due to the elimination of hemicellulose and lignin (Ampofo *et al.* 2021).

CONCLUSION

The results of the presence study indicated that pyrolysis temperature has significate influence on the characteristics of the biochar. however, biochar produced at higher temperature exhibited stable properties such as higher pH, EC, CEC, SSA, and stable carbon content. And this type of biochar has greater impact on soil for agricultural purpose, carbon sequestration, as well as an adsorbent for remediation of organic and inorganic of polluted soil and water environments.

REFERENCES

Adekanye, T., Dada, O. and Kolapo, J. 2022. Pyrolysis of maize cob at different temperatures for biochar production : Proximate, ultimate and spectroscopic characterisation. *Res. in Agril. Engg.*, (1): 27–34.

Ahmad, M., Soo, S., Dou, X., Mohan, D., Sung, J., Yang, J. E. and Sik, Y. 2012. Effects of pyrolysis temperature on soybean stover- and peanut shell-derived biochar properties and TCE adsorption in water. *Bioresource Technol.*, **118**: 536–544.

Ali, L., Palamanit, A., Techato, K., Ullah, A., Chowdhury, S. and Phoungthong, K. 2022. Characteristics of Biochars Derived from the Pyrolysis and Co-Pyrolysis of Rubberwood Sawdust and Sewage Sludge for Further Applications. *Sustainability*, **14**(3829): 1–21.

Aller, D., Aller, D., Bakshi, S. and Laird, D.A. 2018. Modified method for proximate analysis of biochars. *J. of Analyt. and Appl. Pyrolysis*, **124**: 335–342.

Almeida, G.C. De, Tarelho, L.A.C., Hauschild, T., Ang, M., Costa, M. and Duss, K.J. 2022. Biochar production from sugarcane biomass using slow pyrolysis : Characterization of the solid fractions. *Chem. Engg. and Processing - Process Intensification*, **179**.

Amen, R., Yaseen, M., Mukhtar, A., Ullah, S., Al-sehemi, A.G., Ra, S., Babar, M., Lai, C., Ibrahim, M., Asif, S., Shehzad, K., Majeed, M. and Bokhari, A. 2020. Lead and cadmium removal from wastewater using eco-friendly biochar adsorbent derived from rice husk, wheat straw, and corncob. *Cleaner Engg. and Technol.*, **1**: 1–11.

Amin, M.T., Alazba, A.A. and Shafiq, M. 2017. Removal of Copper and Lead using Banana Biochar in Batch Adsorption Systems : Isotherms and Kinetic Studies. *Arabian J. for Sci. and Engg.*, pp. 1–12.

Ampofo, E., Id, S., Song, Y., Yu, Y. and Zhuang, H. 2021. Biochars derived from bamboo and rice straw for sorption of basic red dyes. *PLose One*, **16**(7): 1–20.

Aruya, E.I., Yusuf, R.O. and Yusuf, Y.O. 2016. An assessment of crop residue characteristics and factors militating against efficient management in the Ikara local government area of Kaduna state, Nigeria. *Int. Conference on Waste Manage. and The Environ.*, **202**: 1–12.

Askeland, M., Clarke, B. and Paz-ferreiro, J. 2019. Comparative characterization of biochars produced at three selected pyrolysis temperatures from common woody and herbaceous waste streams. *Peer J.*, 1–20.

Azlina, W., Abdul, W., Ghani, K., Mohd, A., Bachmann, R.T., Taufiq-yap, Y.H., Rashid, U. and Al-muhtaseb, A.H. 2013. Biochar production from waste rubber-wood-sawdust and its potential use in C sequestration : Chemical and physical characterization. *Indus. Crops & Prod.*, **44**: 18–24.

Baffi, C. and Cassinari, C. 2010. *Method for the determination of CEC and exchangeable bases in calcareous soils. February 2014*.

Bayu, A., Nandiyanto, D., Oktiani, R. and Ragadhita, R. 2019. How to Read and Interpret FTIR Spectroscope of Organic Material. *Indonesian J. of Sci. & Technol.*, **4**(1): 97–118.

Bera, T., Purakayastha, T.J., Patra, A.K. and Datta, S.C. 2017. Comparative analysis of physicochemical, nutrient, and spectral properties of agricultural residue biochars as influenced by pyrolysis temperatures. *J. of Material Cycles and Waste Manage., October*. https://doi.org/10.1007/s10163-017-0675-4

Biswas, B., Pandey, N., Bisht, Y., Singh, R., Kumar, J. and Bhaskar, T. 2017. Pyrolysis of agricultural biomass residues : Comparative study of corn cob, wheat straw, rice straw and rice husk. *Bioresource Technol. J.*, **237**: 57–63.

Burachevskaya, M., Minkina, T., Bauer, T., Lobzenko, I., Fedorenko, A., Mazarji, M., Sushkova, S., Mandzhieva, S., Nazarenko, A., Butova, V., Wong, M.H. and Rajput, V.D. 2023. Fabrication of biochar derived from different types of feedstocks as an efficient adsorbent for soil heavy metal removal. *Scientific Reports*, pp. 1–14.

Campos, P., Miller, A.Z., Knicker, H., Costa-pereira, M.F., Merino, A., María, J. and Rosa, D. 2020. Chemical, physical and morphological properties of biochars produced from agricultural residues : Implications for their use as soil amendment. *Waste Manage.*, **105**: 256–267.

Cheng, J., Hu, S., Sun, G., Geng, Z. and Zhu, M. 2021. The effect of pyrolysis temperature on the characteristics of biochar, pyroligneous acids, and gas prepared from cotton stalk through a polygeneration process. *Indus. Crops & Prod.*, **170**: 113690.

Coates, J. 2000. Interpretation of Infrared Spectra, A Practical Approach. *Encyclopedia of Analytical Chemistry*, 10815–10837.

Conz, R.F., Abbruzzini, T.F., Andrade, C.A. De, Milori, D.M.B. P. and Cerri, C.E.P. 2017. Effect of Pyrolysis Temperature and Feedstock Type on Agricultural Properties and Stability of Biochars. *Sci. Res. Pub.*, **8**: 914–933.

Cuixia, Y., Yingming, X., Lin, W., Xuefeng, L. and Yuebing, S. 2020. physico-chemical characteristics and lead (II) removal of biochar derived from chicken manure. *Royal Soc. of Chem.*, **10**: 3667–3674.

Dhar *et al.* 2020. Effects of pyrolysis temperature on production and physicochemical characterization of biochar derived from coconut fiber biomass through slow pyrolysis process. *Biomass Conversion and Biorefinery*, pp. 1–17.

Dhyani, V. and Bhaskar, T. 2017. A comprehensive review on the pyrolysis of lignocellulosic biomass. *Renewable Energy*, https://doi.org/10.1016/j.renene.2017.04.035

El-hassanin, A.S., Samak, M.R., Radwan, S.R. and El-chaghaby, G.A. 2020. Preparation and Characterization of Biochar from Rice Straw and Its Application in Soil Remediation. *Environment and Natural Resources J.*, **18**(3): 283–289.

Ertugay, N. and Malkoc, E. 2014. Adsorption Isotherm, Kinetic, and Thermodynamic Studies for Methylene Blue from Aqueous Solution by Needles of *Pinus sylvestris* L. *Pol. J. Environ. Stud.*, **23**(6): 1995–2006.

Fan, J., Xu, X., Ni, Q., Lin, Q., Shen, X., Lou, L., Fang, J. and Chen, Q. 2018. Enhanced as (V) Removal from Aqueous Solution by Biochar Prepared from Iron-Impregnated Corn Straw. *Hindawi J. of Chem., pp.* 1–8.

Fan, Qian, Z., Liu, J., Geng, N., Hou, J. and Li, D. 2020. Investigation on the adsorption of antibiotics from water by metal loaded sewage sludge biochar. *Water Science & Technology*, pp. 1–12. https://doi.org/10.2166/wst.2020.578

Gaffar, S., Dattamudi, S., Baboukani, A.R., Chanda, S., Novak, J.M., Watts, D.W., Wang, C. and Jayachandran, K. 2021. Physiochemical Characterization of Biochars from Six Feedstocks and Their Effects on the Sorption of Atrazine in an Organic Soil. *Agronomy*, pp. 1–18.

Gao, W., He, W., Zhang, J., Chen, Y., Zhang, Z. and Yang, Y. 2023. Effects of biochar - based materials on nickel adsorption and bioavailability in soil. *Scientific Reports*, pp. 1–16. https://doi.org/10.1038/s41598-023-32502-x

Guo, Zheng, L., Li, Z., Zhou, X., Cheng, S. and Zhang, L. 2021. Effects of various pyrolysis conditions and feedstock compositions on the physicochemical characteristics of cow manure-derived biochar. *J. of Cleaner Prod.*, **311**: 1–10.

Hadey, C., Allouch, M., Alami, M., Boukhlif, F. and Loulidi, I. 2022. Preparation and Characterization of Biochars Obtained from Biomasses for Combustible Briquette Applications. *Hindawi*, pp. 1–13.

Hmid, A., Mondelli, D., Fiore, S., Paolo, F., Al, Z., Dumontet, S., Istituto, C., Mediterraneo, A., Ceglie, V. and Moro, A. 2014a. Production and characterization of biochar from three-phase olive mill waste through slow pyrolysis. *Biomass and Bioenergy*, pp. 2–11.

Hmid, A., Mondelli, D., Fiore, S., Paolo, F., Al, Z., Dumontet, S., Istituto, C., Mediterraneo, A., Ceglie, V. and Moro, A. 2014b. Production and characterization of biochar from three-phase olive mill waste through slow pyrolysis. *Biomass and Bioenergy*, **71**: 330–339.

Hu, X., Zhang, R., Xia, B., Ying, R., Hu, Z., Tao, X. and Yu, H. 2022. Effect of Pyrolysis Temperature on Removal Efficiency and Mechanisms of Hg (II), Cd (II), and Pb (II) by Maize Straw Biochar. *Sustainability*, pp. 1–16.

Huang, H., Reddy, N. G., Huang, X., Chen, P., Wang, P., Zhang, Y., Huang, Y., Lin, P. and Garg, A. 2021. Effects of pyrolysis temperature, feedstock type and compaction on water retention of biochar amended soil. *Scientific Reports*, pp. 1–19.

Jiang, S., Sheng, G. and Jiang, H. 2019. Advances in the characterization methods of biomass pyrolysis products. *Sustainable Chemistry and Engineering*, pp. 1–62. https://doi.org/10.1021/acssuschemeng.9b00868

Kammann, C., Ippolito, J., Hagemann, N., Borchard, N., Cayuela, L., Estavillo, J. M., Fuertes-mendizabal, T., Jeffery, S., Kern, J., Novak, J., Rasse, D., Saarnio, S., Schmidt, H., Spokas, K., Wrage-mönnig, N., Kammann, C., Ippolito, J., Hagemann, N., Borchard, N., … Rasse, D. (2017). *Biochar as a tool to reduce the agricultural greenhouse-gas burden – knowns, unknowns and future research needs TRIAL as. 6897* (June). https://doi.org/10.3846/16486897.2017.1319375

Keerthanan, S., Bhatnagar, A., Mahatantila, K. and Jayasinghe, C. 2020. Engineered tea-waste biochar for the removal of caffeine, a model compound in pharmaceuticals and personal care products (PPCPs), from aqueous media.

Environmental Technology & Innovation, **19**: 100847. https://doi.org/10.1016/j.eti.2020.100847

Khawkomol, S., Neamchan, R., Thongsamer, T. and Vinitnantharat, S. 2021. Potential of Biochar Derived from Agricultural Residues for Sustainable Management. *J. of Sustainability*, **13**(8147): 1–14.

Le *et al.* 2021. Preparation and Characterization of Biochar Derived from Agricultural By-Products for Dye Removal. *Adsorption Science & Technology*, 14.

Liu and Fan, S. 2018. Removal of cadmium in aqueous solution using wheat straw biochar : effect of minerals and mechanism. *Environ. Sci. and Poll. Res.*, pp. 1–13.

Liu, Y., Zhao, X., Li, J., Ma, D. and Han, R. 2012. Characterization of bio-char from pyrolysis of wheat straw and its evaluation on methylene blue adsorption. *Desalination and Water Treatment*, **46**(1–3): 115–123.

Loulidi, I., Boukhlifi, F., Ouchabi, M., Amar, A., Jabri, M., Kali, A., Chraibi, S., Hadey, C. and Aziz, F. 2020. Adsorption of Crystal Violet onto an Agricultural Waste Residue : Kinetics, Isotherm, Thermodynamics, and Mechanism of Adsorption. *Scientific Worrld J., pp.* 1–9.

Mahanty, B. and Mondal, S. 2021. Synthesis of Magnetic Biochar Using Agricultural Waste for the Separation of Cr (VI) From Aqueous Solution. *Arabian Journal for Science and Engineering*, pp. 1–16. https://doi.org/10.1007/s13369-021-05572-0

Mary, G.S., Niveditha, P.S.S. and Mary, G.S. 2016. Production, characterization and evaluation of biochar from pod (*Pisum sativum*), leaf (*Brassica oleracea*) and peel (*Citrus sinensis*) wastes. *Int. J. of Recycling of Organic Waste in Agric.*, **5**(1): 43–53.

Mubarik, S., Saeed, A., Athar, M.M. and Iqbal, M. 2015. Characterization and mechanism of the adsorptive removal of 2, 4, 6-trichlorophenol by biochar prepared from sugarcane baggase. *Journal of Industrial and Engineering Chemistry*. https://doi.org/10.1016/j.jiec.2015.09.029

Munar-florez, D.A., Varón-cardenas, D.A., Ramírez-contreras, N.E. and García-núñez, J.A. 2021. Adsorption of ammonium and phosphates by biochar produced from oil palm shells : Effects of production conditions. *Results in Chemistry*, **3**: 1–12.

Naeem, M.A., Imran, M., Amjad, M., Abbas, G., Tahir, M., Murtaza, B., Zakir, A., Shahid, M., Bulgariu, L. and Ahmad, I. 2019. Batch and Column Scale Removal of Cadmium from Water Using Raw and Acid Activated Wheat. *Water*, pp. 1–17.

Natrayan, L., Kaliappan, S., Dheeraj, C.N., Reddy, K., Karthick, M., Sivakumar, N.S., Patil, P.P., Sekar, S. and Thanappan, S. 2022. Development and Characterization of Carbon-Based Adsorbents Derived from Agricultural Wastes and Their Effectiveness in Adsorption of Heavy Metals in Waste Water. *Bioinorganic Chemistry and Applications*, *2022*.

Nazari, S., Rahimi, G., Khademi, A. and Nezhad, J. 2019. Effectiveness of native and Citric Acid-enriched biochar of Chickpea straw in Cd and Pb sorption in an acidic soil. *Biochemical Pharmacology*, pp. 1–25. https://doi.org/10.1016/j.jece.2019.103064

Nguyen, T.H., Pham, T.H., Tham, H., Thi, N., Nguyen, T.N., Nguyen, M., Dinh, T.T., Nguyen, M.P., Do, T.Q., Phuong, T., Hoang, T.T., Tung, T., Hung, M., Ha, V. and Thi, T. 2019. Synthesis of Iron-Modified Biochar Derived from Rice Straw and Its Application to Arsenic Removal. *J. of Chem., 2019*, 8.

Novak, J. 2014. Production and characterization of biochars from agricultural by-products for use in soil quality enhancement. *Journal of Analytical and Applied Pyrolysis Production and characterization of biochars from agricultural by-products for use in soil quality enh. November 2017*. https://doi.org/10.1016/j.jaap.2014.03.008

Oyegoke, T., Oyegoke, A.F., Fasanya, O. and Abdul-alim, I. 2023. *State of Agro-wastes Management in Nigeria : Status, Implications & Way Forward* (Issue May).

Poo, K., Son, E., Chang, J., Ren, X., Choi, Y. and Chae, K. 2018. Biochars derived from wasted marine macro-algae (*Saccharina japonica* and *Sargassum fusiforme*) and their potential for heavy metal removal in aqueous solution. *J. of Environ. Mgt.*, **206**: 364–372.

Reyhanitabar, A., Farhadi, E. and Ramezanzadeh, H. 2020. Effect of Pyrolysis Temperature and Feedstock Sources on Physicochemical Characteristics of Biochar. *J. of Agr. Sci. Tech.*, **22**(2): 547–561.

Sahoo, S.S., Vijay, V.K., Chandra, R. and Kumar, H. 2021a. Production and characterization of biochar produced from slow pyrolysis of pigeon pea stalk and bamboo. *Cleaner Engineering and Technology*, **3**: 1–10.

Sahoo, S.S., Vijay, V.K., Chandra, R. and Kumar, H. 2021b. Production and characterization of biochar produced from slow pyrolysis of pigeon pea stalk and bamboo. *Cleaner Engineering and Technology*, **3**: 1–11.

Sarfaraz, Q., Souza, L., Drescher, G.L., Zafar, M., Shafique, Q. and Solaiman, Z.M. 2020. Characterization and carbon mineralization of biochars produced from different animal manures and plant residues. *Scientific Reports*, 2–10. https://doi.org/10.1038/s41598-020-57987-8

Shi, J., Fan, X., Tsang, D.C.W., Wang, F., Shen, Z., Hou, D. and Alessi, D.S. 2019. Removal of lead by rice husk biochars produced at different temperatures and implications for their environmental utilizations. *Chemosphere*, **235**: 825–831.

Singh, V., Pant, N., Sharma, R.K., Padalia, D. and Rawat, P.S. 2023. Adsorption Studies of Pb (II) and Cd (II) Heavy Metal Ions from Aqueous Solutions Using a Magnetic Biochar Composite Material Adsorption Studies of Pb (II) and Cd (II) Heavy Metal Ions from. *Separation Science and Technology*, **10**(389): 1–17.

Song, Cong, P., Wang, C., Li, P., Liu, S., He, Z., Zhou, C. and Liu, Y. 2023. Properties of Biochar Obtained from Tropical Crop Wastes Under Different Pyrolysis Temperatures and Its Application on Acidic Soil Properties of Biochar Obtained from Tropical Crop Wastes Under Different Pyrolysis Temperatures and Its Application on Acid. *Agronomy*, pp. 1–15.

Song, W. and Guo, M. 2012. Quality variations of poultry litter biochar generated at different pyrolysis temperatures. *J. of Analytical and Appl. Pyrolysis*, **94**: 138–145.

Steiner, C., Novak, J.M., Lima, I., Gaskin, J.W., Steiner, C., Das, K.C. and Ahmedna, M. 2009. Characterization of Designer Biochar Produced at Different Temperatures and Their Effects on a Loamy Sand. *Annals of Environ. Sci.*, **3**: 195–206.

Sun, Gao, B., Yao, Y., Fang, J., Zhang, M., Zhou, Y., Chen, H. and Yang, L. 2014. Effects of feedstock type, production method, and pyrolysis temperature on biochar and hydrochar properties. *Chem. Engineer. J.*, **240**: 574–578.

Sun, Zhang, G., Li, X., Zhang, X. and Hang, W. 2023. Effects of biochar on the transformation of cadmium fractions in alkaline soil. *Heliyon*, **9**(1): e12949.

Tong, X., Li, J., Yuan, J. and Xu, R. 2011. Adsorption of Cu (II) by biochars generated from three crop straws. *Chem. Engineer. J.*, pp. 828–834.

Tran, H.N., You, S. and Chao, H. 2016. Effect of pyrolysis temperatures and times on the adsorption of cadmium onto orange peel derived biochar. *Waste Manage.*, **34**(2): 129–138.

Tripathi, M., Sahu, J.N. and Ganesan, P. 2016. Effect of process parameters on production of biochar from biomass waste through pyrolysis : A review. *Renewable and Sustainable Energy Rev.*, **55**: 467–481.

Ullah, A., Zahoor, M., Din, W.U., Muhammad, M., Khan, F.A., Sohail, A., Ullah, R., Ali, E.A. and Murthy, H.C.A. 2022. Removal of Methylene Blue from Aqueous Solution Using Black Tea Wastes : Used as Efficient Adsorbent. *Hindawi Adsorption Science & Technol., pp.* 1–9.

Venkatesh, G., Venkateswarlu, B., Gopinath, K.A., Srinivasrao, C., Korwar, G.R. and Sanjeeva, B. 2013. Biochar Production Technology for Conversion of Cotton Stalk Bioresidue into Biochar and its Characterization for Soil Amendment Qualities. *Indian J. Agric.*, **28**(1): 48–57.

Videgain-marco, M., Marco-montori, P., Mart, C. and Josep, J. 2020. E ffects of Biochar Application in a Sorghum Crop under Greenhouse Conditions : Growth Parameters and Physicochemical Fertility. *Agronomy*, pp. 1–17.

Wahi, R., Mona, S., Aziz, A., Hamdan, S. and Ngaini, Z. 2015. Biochar Production from Agricultural Wastes via Low-Temperature Microwave Carbonization. *Conference*, *04*(August 2017). https://doi.org/10.1109/RFM.2015.7587754

Wang, Chi, Q., Liu, X. and Wang, Y. 2018. Influence of pyrolysis temperature on characteristics and environmental risk of heavy metals in pyrolyzed biochar made from hydrothermally treated sewage sludge. *Chemosphere*, pp. 1–38. https://doi.org/10.1016/j.chemosphere.2018.10.189

Weber, K. and Quicker, P. 2018. Properties of biochar. *Fuel*, **217**: 240–261.

Wei, S., Zhu, M., Fan, X., Song, J., Li, K., Jia, W. and Song, H. 2019. Influence of pyrolysis temperature and feedstock on carbon fractions of biochar produced from pyrolysis of rice straw, pine wood, pig manure and sewage sludge. *Chemosphere*, **218**: 624–631.

Wu, Xian, Y., He, Z., Zhang, Q., Wu, J., Yang, G. and Zhang, X. 2019. Adsorption characteristics of Pb (II) using biochar derived from spent mushroom substrate. *Scientific Reports*, *Ii*, pp. 1–11. https://doi.org/10.1038/s41598-019-52554-2

Wystalska, K., Kwarciak, A. and Renata, W. 2023. Influence of Technical Parameters of the Pyrolysis Process on the Surface Area, Porosity, and Hydrophobicity of Biochar from Sunflower Husk Pellet. *Sustainability*, pp. 1–13.

Wystalska, K. and Meers, E. 2021. Influence of Pyrolysis Temperature on the Heavy Metal Sorption Capacity of Biochar from Poultry Manure. *Materials*, **14**: 1–21.

Xiaoling, Song, J., Wang, H., Zhang, W., Wang, B., Lyu, W., Wang, Q., Liu, P., Chen, L. and Xing, J. 2020. Adsorption of Cr(VI) and Cu(II) from aqueous solutions by biochar derived from *Chaenomeles sinensis* seed. *J. of Water Sci. and Technol.*, pp. 1–13. https://doi.org/10.2166/wst.2020.036

Xiaoxiao, Zhang, P., Yuan, X., Li, Y. and Han, L. 2019. Effect of pyrolysis temperature and correlation analysis on the yield and physicochemical properties of crop residue biochar. *Bioresource Technology*, 122318. https://doi.org/10.1016/j.biortech.2019.122318

Xing, X., Fan, F. and Jiang, W. 2018. Characteristics of biochar pellets from corn straw under different pyrolysis temperatures. *Royal Society Open Science*, pp. 1–10.

Yaoyao, Dong, H., Li, L., Tian, R., Chen, J., Ning, Q., Wang, B., Tang, L. and Zeng, G. 2019. Influence of feedstocks and modification methods on biochar's capacity to activate hydrogen peroxide for tetracycline removal. In *Bioresource Technology*. Elsevier Ltd. https://doi.org/10.1016/j.biortech.2019.121840

Zhang, P., Zhang, X., Li, Y. and Han, L. 2020. Influence of pyrolysis temperature on chemical speciation, leaching ability, and environmental risk of heavy metals in biochar derived from cow manure. *Bioresource Technology*, 122850. https://doi.org/10.1016/j.biortech.2020.122850

Zhang, Xiaoxiao, Yang, X., Yuan, X., Tian, S., Wang, X., Zhang, H. and Han, L. 2022. Effect of pyrolysis temperature on composition, carbon fraction and abiotic stability of straw biochars : correlation and quantitative analysis. *Carbon Res.*, **1**(17): 1–14.

Zhang, Xin, Zhao, B., Liu, H., Zhao, Y. and Li, L. 2022. Effects of pyrolysis temperature on biochar's characteristics and speciation and environmental risks of heavy metals in sewage sludge biochars. *Environ. Technol. & Innovation*, **26**: 1–11.

Zhang, Zhang, K., Li, Y., Kang, Q., Wang, Y., Wang, J., Yang, K., Zhang, K., Zhang, K., Li, Y., Kang, Q., Wang, Y., Wang, J. and Yang, K. 2023. Easily Pyrolyzable Biomass Components Significantly Affect the Physicochemical Properties and Water-Holding Capacity of the Pyrolyzed Biochar the Physicochemical Properties and Water-Holding Capacity. *Agriculture Article*, pp. 1–14.

Zhao, S., Ta, N. and Wang, X. 2017. Effect of Temperature on the Structural and Physicochemical Properties of Biochar with Apple Tree Branches as Feedstock Material. *Energies*, pp. 1–15. https://doi.org/10.3390/en10091293

Zhaoxia Liu, Wenjuan Niu, Heying Chu, Tan Zhou, and Z. N. 2018. Effect of the Carbonization Temperature on the Properties of Biochar Produced from the Pyrolysis of Crop Residues. *Bioresources*, **13**(2): 3429–3446.

Zhenyu, Zheng, H., Luo, Y., Deng, X., Herbert, S. and Xing, B. 2013. Characterization and influence of biochars on nitrous oxide emission from agricultural soil. *Environmental Pollution*, **174**: 289–296.